



## Article

# Genome-Wide Identification of Superoxide Dismutase and Expression in Response to Fruit Development and Biological Stress in *Akebia trifoliata*: A Bioinformatics Study

Huai Yang<sup>1</sup>, Qiuyi Zhang<sup>1</sup>, Shengfu Zhong<sup>1</sup>, Hao Yang<sup>1</sup>, Tianheng Ren<sup>1</sup> , Chen Chen<sup>1</sup>, Feiquan Tan<sup>1</sup>, Guoxing Cao<sup>2</sup> , Jun Liu<sup>2</sup> and Peigao Luo<sup>1,\*</sup>

<sup>1</sup> Key Laboratory of Plant Genetics and Breeding, Sichuan Agricultural University of Sichuan Province, Chengdu 611130, China

<sup>2</sup> College of Forestry, Sichuan Agricultural University, Chengdu 611130, China

\* Correspondence: lpglab@sicau.edu.cn

**Abstract:** *Akebia trifoliata* is a newly domesticated perennial fruit tree, and the lack of molecular research on stress resistance seriously affects its genetic improvement and commercial value development. Superoxide dismutase (SOD) can effectively eliminate the accumulation of reactive oxygen species (ROS) during the rapid growth of plant organs under biotic and abiotic stresses, maintaining a steady state of physiological metabolism. In this study, 13 SODs consisting of two FeSODs (FSDs), four MnSODs (MSDs) and seven Cu/ZnSODs (CSDs) were identified in the *A. trifoliata* genome. Structurally, the phylogeny, intron–exon pattern and motif sequences within these three subfamilies show high conservation. Evolutionarily, segmental/wide genome duplication (WGD) and dispersed duplication form the current SOD profile of *A. trifoliata*. Weighted gene coexpression network analysis (WGCNA) revealed the metabolic pathways of nine (69.2%) SODs involved in fruit development, among which *AktMSD4* regulates fruit development and *AktCSD4* participates in the stress response. In addition, under the stress of multiple pathogens, six (46.6%) SODs were continuously upregulated in the rinds of resistant lines; of these, three SODs (*AktMSD1*, *AktMSD2* and *AktMSD3*) were weakly or not expressed in susceptible lines. The results pave the way for theoretical research on SODs and afford the opportunity for genetic improvement of *A. trifoliata*.

**Keywords:** *Akebia trifoliata*; superoxide dismutase; fruit development; biotic stress; expression profile



**Citation:** Yang, H.; Zhang, Q.; Zhong, S.; Yang, H.; Ren, T.; Chen, C.; Tan, F.; Cao, G.; Liu, J.; Luo, P. Genome-Wide Identification of Superoxide Dismutase and Expression in Response to Fruit Development and Biological Stress in *Akebia trifoliata*: A Bioinformatics Study. *Antioxidants* **2023**, *12*, 726. <https://doi.org/10.3390/antiox12030726>

Academic Editors: Francisco J. Corpas and José M. Palma

Received: 22 February 2023

Revised: 7 March 2023

Accepted: 14 March 2023

Published: 15 March 2023



**Copyright:** © 2023 by the authors. Licensee MDPI, Basel, Switzerland. This article is an open access article distributed under the terms and conditions of the Creative Commons Attribution (CC BY) license (<https://creativecommons.org/licenses/by/4.0/>).

## 1. Introduction

Reactive oxygen species (ROS), including superoxide radicals ( $O_2^{\cdot-}$ ), hydroxyl radicals ( $\cdot OH$ ) and hydrogen peroxide ( $H_2O_2$ ), are inevitable byproducts of biological oxidation reactions in plant cells [1], and the production of ROS is further intensified when plants are subjected to biotic and abiotic stresses [2–4]. On the one hand, accumulated ROS can act as signaling molecules to regulate the expression of downstream genes to cope with adversity [5]. On the other hand, excessively accumulated ROS can damage plant cell membranes, destroy biological macromolecules, and even cause cell death [1]. In response to the toxic mechanism of ROS, plants have evolved a set of sophisticated antioxidant enzyme systems to maintain ROS homeostasis in cells [6], among which superoxide dismutase (SOD) is the first line of defense [7]. Therefore, to explore the molecular mechanism of plant stress tolerance, many scholars have carried out much research on the structure, function and phylogeny of plant SOD genes [8,9].

The SOD gene family is a class of metal-binding enzymes. Plant SOD genes are divided into three groups according to metal cofactors: iron SOD (FeSOD), manganese SOD (MnSODs) and copper/zinc SOD (Cu/ZnSOD) [10]. Another type of SOD, nickel SOD (NiSOD), exists mainly in bacteria, and has not been detected in plants [11]. In terms of the three subfamilies in plants, the subcellular localization of SOD proteins is usually

related to the production site of  $O_2^{\cdot-}$ . The compartmentalization of SOD proteins in the cell organelles is extremely important for plant response to oxidation stress induced by abiotic factors and cell signal transformation [12]. Evolutionarily, *FeSODs* and *MnSODs* have ancient origins and are present in bacteria, protozoa, and primitive algae [13]. It is generally believed that *FeSODs* and *MnSODs* have a common ancestor due to their striking similarities [14]. The separate evolution of *FeSODs* and *MnSODs* may be related to changes in oxygen levels on early Earth [13]. For example, the specific Mn/*FeSODs* in a few archaea, such as *Aeropyrum pernix* and *Pyrobaculum calidifontis*, are active with Fe but prefer to bind Mn, especially under aerobic conditions [15,16]. In addition, *Cu/ZnSODs* in plants are considered to have evolved separately from other *SODs* because to date, *Cu/ZnSOD* has not been detected in primitive plants such as *Chlamydomonas* or mosses [13,17].

A large number of reports have confirmed that the inducible expression of *SOD* helps plants respond to abiotic and biotic stresses. For example, the *SOD* activity of salt-tolerant varieties of *Brassica napus* is higher than that of salt-sensitive varieties under salt stress [18]. Under cold stress, the ROS content of cold-tolerant tea tree varieties is higher than that of cold-sensitive varieties, resulting in less damage to the leaves of the former [19]. Furthermore, the plant immune system relies on *SODs* to precisely regulate ROS content, to mediate the immune response to invading pathogenic bacteria. For example, after transferring the tomato *SOD* gene into sugarbeet, the transgenic lines showed strong resistance to oxidative agents as well as the fungus *Cercospora beticola* [20]. In addition to responding to biotic and abiotic stresses, changes in expression and enzyme activity of *SOD* genes during apple fruit ripening suggest that *SOD* plays an important role in fruit development [21,22].

*Akebia trifoliata* (Thunb.) Koidz., is a newly domesticated perennial woody vine with a high commercial development value. The root, stem and unripe fruit of *A. trifoliata* have been used as Chinese medicinal materials for thousands of years [23]. In recent years, *A. trifoliata* has been planted in a large area in Southwest China because of its delicious fruit pulp and high-quality seed oil [24,25]. However, genetic improvement of *A. trifoliata* is still in its infancy due to the short time of development and utilization, especially in terms of resistance to biotic and abiotic stresses. Therefore, improving tolerance of *A. trifoliata* to biotic and abiotic stresses is an urgent task for breeders.

*SOD* and *nucleotide binding sites (NBS)* genes are two major means by which plants resist abiotic and biotic stresses [1,26]. To date, the *NBS* gene family in *A. trifoliata* has been systematically identified and analyzed [27], but *SOD* genes have not yet been reported. To speed up theoretical research on adversity stress of *A. trifoliata* to promote progress in commercial exploitation, we systematically identified and analyzed the *SOD* genes of *A. trifoliata* (*AktSOD*), including gene structure, conserved motifs, homology and phylogenetic developmental relationships, based on its published high-quality reference genome. Based on the reported transcriptome data, the expression characteristics of *SOD* genes were also revealed during the fruit development of *A. trifoliata* and critical stage of resisting pathogen invasion, which will help us to initially explore the role of *AktSOD* genes in fruit development and resistance to biotic stress.

## 2. Materials and Methods

### 2.1. Identification and Analysis of *AktSOD* Genes in *A. trifoliata*

Genome sequence, protein sequence and annotation files of *A. trifoliata* downloaded from the National Genomics Data Center database under BioProject PRJCA003847 were employed to identify and analyze *SOD* genes. To identify *SOD*-encoding proteins, hidden Markov model (HMM) *Cu/ZnSOD* (PF00080) and *Fe-MnSOD* (PF02777 and PF00081) files downloaded from the Pfam database (<http://smart.embl.de/smart/batch.pl>, accessed on 28 December 2022) were used to filter protein sequences of *A. trifoliata* with the  $1 \times 10^{-5}$  e-value parameter [28]. The domains of candidate *AktSOD* proteins were further verified using Conserved Domain Database (CDD) at the National Center for Biotechnology Information (NCBI) (<https://www.ncbi.nlm.nih.gov/cdd/>, accessed on 3 January 2023). The

molecular weight (MW) and theoretical isoelectric point (pI) of proteins were computed via ExPasy (<https://www.expasy.org/>, accessed on 3 January 2023). Subcellular localization was predicted by the online website Plant-mPLOC (<http://www.csbio.sjtu.edu.cn/bioinf/plant-multi/>, accessed on 3 January 2023). Conserved *AktSOD* protein sequence motifs were analyzed by MEME Suite (<https://meme-suite.org/meme/tools/meme>, accessed on 5 January 2023). To constberruct the phylogenetic relationship of *AktSOD* protein sequences, after multiple alignments of the *SOD* protein sequences using ClustalW (Kyoto University Bioinformatics Center, Japan) [29], a phylogenetic tree was constructed and drawn by the maximum likelihood method using MEGA 11 software with 1000 bootstrap replicates [29]. Finally, integrated mapping of the *AktSOD* protein structure, conserved motifs and intron–exon pattern was performed using TBtools software (version 1.0876, CJ chen, Guangzhou, China) [30].

## 2.2. Phylogenetic Tree Construction of Plants at Different Evolutionary Nodes

*SOD* protein sequences of *Amborella trichopoda* (basal angiosperm), *Aquilegia coerulea* (basal dicot), *Arabidopsis thaliana* (core dicot), and *Oryza sativa* (monocotyledon) were identified in the same way as those of *A. trifoliata*. The protein sequences of *A. trichopoda* and *A. coerulea* were downloaded from NCBI; those of *A. thaliana* and *O. sativa* were downloaded from Ensembl Plants (<http://plants.ensembl.org/index.html>, accessed on 6 January 2023). The evolutionary relationship was constructed using IQtree with 1000 bootstrap replicates [31], and the online tool iTOL (<https://itol.embl.de/>, accessed on 15 January 2023) was used for subsequent visualization [32].

## 2.3. Synteny, Replication and Chromosomal Distribution Analysis of *AktSOD* Genes

Synteny and replication analysis of *AktSOD* genes was performed using the MCScanX module of TBtools software [30]. Information regarding the physical location of *AktSOD* genes was obtained from the annotation file of the *A. trifoliata* genome. Then, chromosomal distribution and collinearity mapping of *AktSOD* genes were called using the Circos Gene View module of TBtools [30].

## 2.4. Cis-Acting Elements of the *AktSOD* Gene Family

To predict putative cis-acting elements in *AktSOD* gene promoters, the 2000 bp upstream sequence of *AktSOD* gene coding regions was analyzed using PlantCARE (<http://bioinformatics.psb.ugent.be/webtools/plantcare/html/>, accessed on 10 January 2023) [33]. A heatmap of the quantity statistics results was prepared using the HeatMap module of TBtools [30].

## 2.5. Expression Analysis of *AktSOD* Genes in Fruit Development and Rinds at Different Disease Resistance Levels

Transcriptome data for *A. trifoliata* fruit tissues (flesh, rind and seeds) at four developmental stages (young, enlargement, coloring and maturity) were downloaded from the NCBI database (accession IDs: SAMN16551931-33, young stage; SAMN16551934-36, enlargement stage; SAMN16551937-39, coloring stage; SAMN16551940-42, mature stage). Transcriptome data for both the mixed pool of 24 lines exhibiting resistance and another mixed pool of 50 lines exhibiting susceptibility to fungal disease at three different developmental stages were also downloaded from the National Genomics Data Center database under BioProject PRJCA014987. First, transcriptome reads were aligned to the *A. trifoliata* reference genome using HISAT2 software with default parameters [34]. Second, fragments per kilobase of transcript per million fragments mapped (FPKM) values calculated by ESeq2 were used to estimate gene expression levels [35]. Finally, the expression level of *AktSOD* genes was converted to a heatmap by TBtools [30].

## 2.6. WGCNA of the Fruit Development Transcriptome

To investigate the metabolic network in which *AktSOD* genes may participate, 12 transcriptome sets consisting of three fruit tissues at four developmental stages were subjected to weighted gene coexpression network analysis (WGCNA) using the WGCNA shiny plugin of TBtools [30]. A total of 12,016 genes were included in the analysis after filtering out genes with FPKM < 1. Other analysis-related parameters were as follows: R<sup>2</sup> cutoff = 0.85, module size = 30, and module cutree height = 0.25.

## 2.7. GO Annotation Analysis

Genes in the transcriptome during fruit development were divided into 18 modules by WGCNA. We determined the set of genes expressed in association with the *AktSOD* genes from the module where the genes are located. These gene sets were further subjected to Gene Ontology (GO) annotation analysis via the eggNOG website (<http://eggno-mapper.embl.de/>, accessed on 20 January 2023) [36]. The GO Enrichment module of TBtools was used to perform GO enrichment analysis [30].

## 3. Results

### 3.1. Genome-Wide Identification of the SOD Gene Family in *A. trifoliata*

In this study, a total of 13 SOD genes were identified in the *A. trifoliata* genome through HMM analysis and domain validation (Table 1). These 13 SOD genes were renamed *AktFSD1*, *AktFSD2*, *AktMSD1–AktMSD4*, and *AktCSD1–AktCSD7* according to metal factor type and chromosomal position. The length of the open reading frame of *AktSOD* genes varies greatly, from 2569 bp to 25,161 bp. The results showed that the sequence lengths of the 13 *AktSOD* proteins range from 120 (*AktCSD7*) to 329 (*AktCSD5*) aa, the molecular weights from 12.730 (*AktCSD7*) to 35.181 (*AktCSD5*) kDa, and the isoelectric points from 4.95 (*AktFSD2*) to 9.02 (*AktMSD2*) kDa. According to the prediction of subcellular localization, the products of the two *FeSOD* genes localize to mitochondria (*AktFSD1*) and chloroplasts (*AktFSD2*), those of the 4 *MnSOD* genes to mitochondria, those of the 7 *Cu/ZnSOD* to chloroplasts, and those of *AktCSD2* and *AktCSD7* to the cytoplasm.

**Table 1.** Characteristics of the SOD gene families identified in the *A. trifoliata* genome.

Name	Gene ID	SOD Type	AA	pI	MW (kDa)	Number of Exon	Number of Intron	Duplication Type	Subcellular Localization
<i>AktCSD1</i>	EVM0009170	Cu/ZnSOD	152	5.66	15.362	8	7	WGD/Segmental	Chloroplas.
<i>AktCSD2</i>	EVM0011294	Cu/ZnSOD	160	6.79	23.238	7	6	Dispersed	Chloroplast, Cytoplasm
<i>AktCSD3</i>	EVM0015107	Cu/ZnSOD	169	5.27	17.118	8	7	WGD/Segmental	Chloroplast
<i>AktCSD4</i>	EVM0004711	Cu/ZnSOD	214	6.39	21.895	8	7	WGD/Segmental	Chloroplast
<i>AktCSD5</i>	EVM0014685	Cu/ZnSOD	329	5.36	35.181	7	6	Dispersed	Chloroplast
<i>AktCSD6</i>	EVM0003060	Cu/ZnSOD	223	6.79	23.238	8	7	WGD/Segmental	Chloroplast
<i>AktCSD7</i>	EVM0005862	Cu/ZnSOD	120	6.2	12.730	6	5	WGD/Segmental	Chloroplast, Cytoplasm
<i>AktFSD1</i>	EVM0017725	FeSOD	205	7.11	24.065	8	7	Dispersed	Mitochondrion
<i>AktFSD2</i>	EVM0016720	FeSOD	301	4.95	34.734	9	8	Dispersed	Chloroplast
<i>AktMSD1</i>	EVM0002565	MnSOD	171	7.89	18.538	7	6	Dispersed	Mitochondrion
<i>AktMSD2</i>	EVM0008804	MnSOD	147	9.02	16.154	5	4	Dispersed	Mitochondrion
<i>AktMSD3</i>	EVM0020914	MnSOD	158	7.78	17.433	5	4	Dispersed	Mitochondrion
<i>AktMSD4</i>	EVM0011812	MnSOD	243	8.38	27.293	6	5	Dispersed	Mitochondrion

Abbreviations: AA, the number of amino acids; pI, isoelectric point; MW, theoretical subunit size of the proteins.

### 3.2. Phylogenetic Classification of AktSODs in Plants at Different Evolutionary Nodes

To clarify the evolutionary relationship and the classification of *AktSOD* gene subfamilies, 38 reference SOD protein sequences from plants at different evolutionary nodes (Table S1), including 7 SODs of *A. trichopoda* (basal angiosperm), 11 SODs of *A. coerulea* (basal dicot), 9 SODs of *A. thaliana* (core dicot), 11 SODs of *O. sativa* (monocotyledon) and 13 SODs of *A. trifoliata*, were used to construct a phylogenetic tree. In the phylogenetic tree (Figure 1), all 30 *Cu/ZnSOD* genes in the 5 species grouped into one group, all 6 *MnSOD*

genes and 12 *FeSOD* genes grouped into another group. Interestingly, the *SODs* of *A. trifoliata* frequently clustered with the *SODs* of *A. coerulea*.

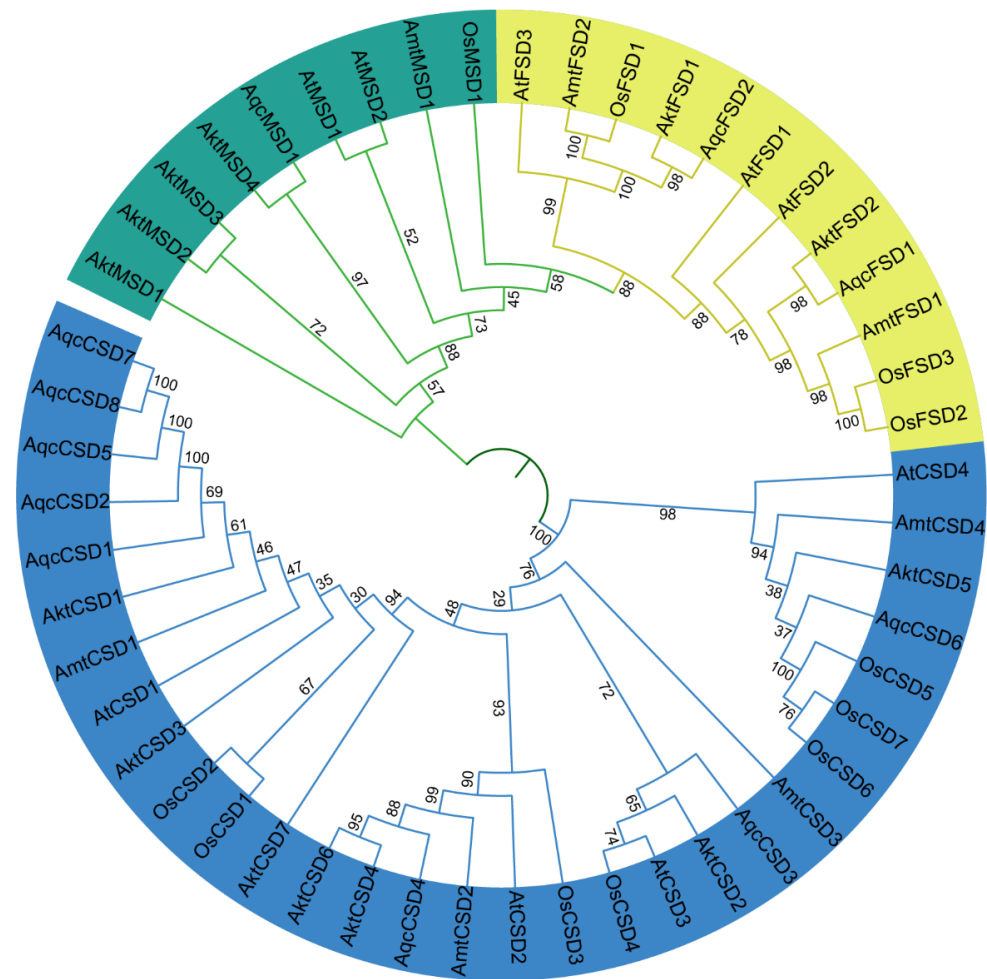


**Figure 1.** Phylogenetic tree of *SOD* genes from 4 plants: *A. trichopoda*, *A. coerulea*, *A. thaliana* and *O. sativa* (the numbers at nodes indicates bootstrap numbers per 1000 replicates determined by maximum likelihood methods).

### 3.3. Phylogeny and Conserved Motifs of *AktSOD* Genes

The 13 *AktSODs* were divided into two groups in the phylogenetic tree (Figure 2a): 7 *Cu/ZnSODs* were classified into one group; the other 6, consisting of 2 *FeSODs* and 4 *MnSODs*, were classified into another group. Identification of conserved domains indicated that the 2 *Akt-FeSODs* and 4 *Akt-MnSODs* have similar domain compositions, with both containing an *Sod\_Fe\_C* and *Sod\_Fe\_N* domain. In contrast, *Akt-Cu/ZnSODs* have only 1 *Sod\_Cu* domain (Figure 2b). Motif analysis further revealed similarities and differences in the protein sequences of the three subfamilies of *AktSODs*. A total of 10 conserved motifs were identified in the 13 *AktSODs* (Figure 2c, Table S2): motifs 1, 2, 6, and 9 are only present in *Akt-Cu/ZnSODs*; motifs 4, 5, 7, and 10 are common to *Akt-FeSODs* and *Akt-MnSODs*; motif 8 exists only in *Akt-FeSODs*; and motif 3 is unique to *Akt-MnSODs*. Structurally, the coding sequences of the 13 *AktSODs* are separated by multiple introns, with the number of introns ranging from 4 to 8 (Figure 2d; Table 1).

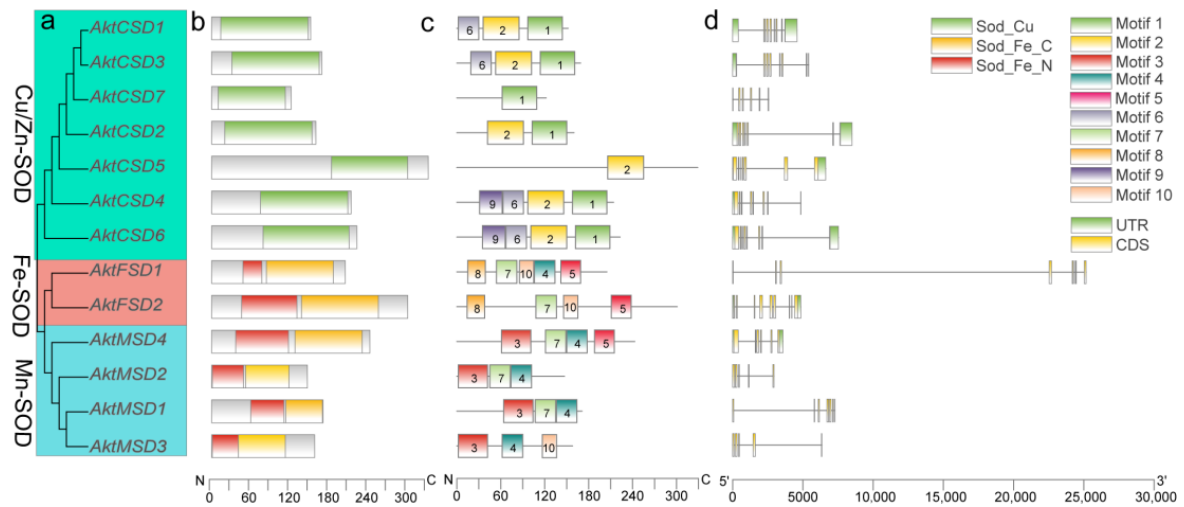


**Figure 2.** Gene and protein structure analyses of *AktSOD* families. (a) Phylogenetic tree of *AktSOD* genes. (b) Conserved domains of *AktSOD* proteins. (c) Motifs of *AktSOD* proteins. (d) Exon–intron structures of *AktSOD* genes.

### 3.4. Chromosomal Distributions and Duplication Types of *AktSODs*

The chromosomal physical locations of the 13 *AktSODs* are depicted in Figure 3. Among the 16 chromosomes of *A. trifoliata*, 9 chromosomes harbor 13 *AktSOD* genes. Chromosomes 5, 6, 9, 10, 13 and 16 each carry an *SOD* gene, chromosomes 3 and 8 both carry 2 *SOD* genes, and chromosome 15 carries the remaining 3 *SOD* genes. Gene duplication analysis of the *AktSOD* family revealed dispersed duplication in 8 *SOD* genes; the other 5 *SOD* genes experienced segmental/wide genome duplication (WGD) (Table 1; Figure 3).

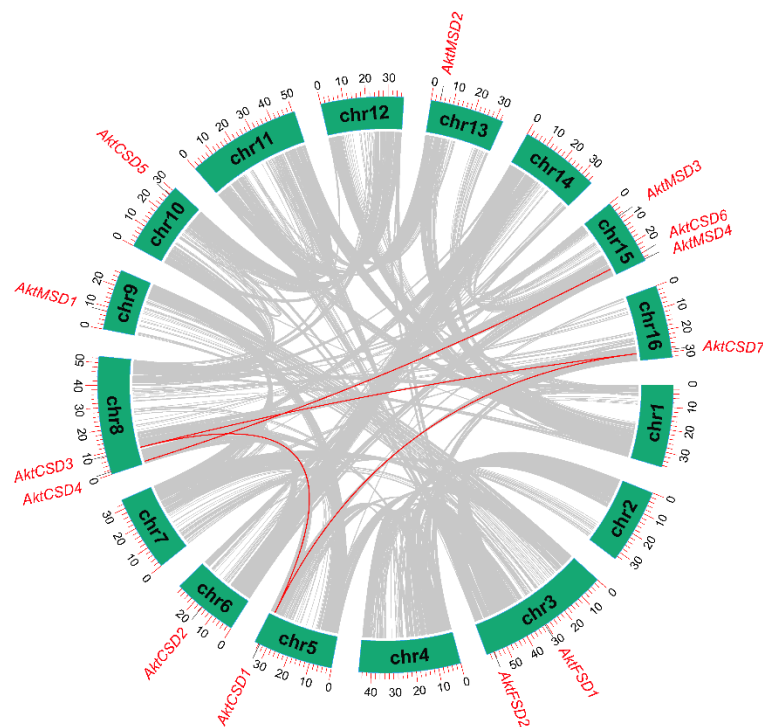


**Figure 3.** Chromosomal localization and interchromosomal synteny of *AktSODs*. Red lines in the inner circle represent syntenic gene pairs from WGD/fragment duplications.

### 3.5. Detection of Cis-Acting Elements in the Promoter Sequence of AktSODs

Statistical results for putative cis-acting elements showed a large number of environmental and hormone-responsive elements to be distributed throughout the promoter region of *AktSODs* (Figure 4; Table S3). All *AktSODs* contain at least one light-responsive, stress-responsive and drought-inducible element. The number of light-responsive elements is greatest; *AktFSD1* has the lowest number, at 5; *AktMSD4* has the highest number, at 20. In addition, 5 plant hormone-responsive elements, including for abscisic acid (ABA), methyl jasmonate (MeJA), gibberellin (GA), salicylic acid (SA) and auxin, were detected in the promoter region of *AktSODs*, with the distribution varying. For example, *AkCSD5* has only one hormone-responsive element, namely, the TCA element, which is annotated as responsive to salicylic acid (Table S3). *AkCSD4*, *AkCSD7*, *AkFSD1*, and *AkMSD2* contain four types of hormone-responsive elements.

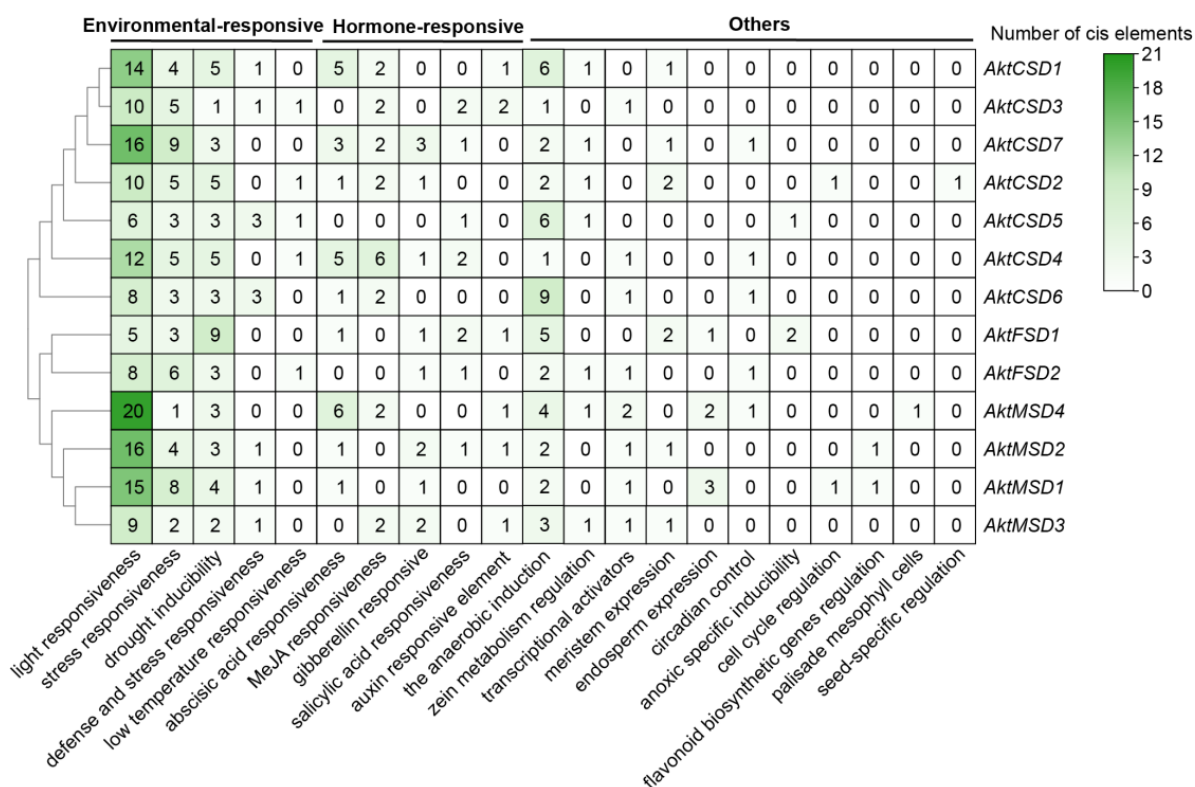


**Figure 4.** Analysis of cis-regulatory elements in the 2 kb region upstream of the transcription start site of *AktSODs*.

### 3.6. Expression Analysis of AktSODs in Different Tissues of *A. trifoliata* Fruit

Based on the expression analysis of *AktSODs* using flesh, seed and rind tissues, the expression of 12 *AktSODs* was detected, with the levels of most being similar in the flesh, seed and rind tissues at four developmental stages (young, enlargement, coloring, and mature stage) (Figure 5a; Table S4). Only the expression of *AktCSD7* could not be detected in any of the samples. In contrast, the expression level of *Cu/ZnSODs* was higher than that of the other two subfamilies of *SODs*; *AktCSD3* showed the highest expression level. Two *FeSODs* (*AktFSD1* and *AktFSD2*) showed persistent low expression levels during the development of flesh, seed and rind tissues. Among the 4 *MnSODs*, *AktMSD4* was continuously expressed at a high level, but *AktMSD2* and *AktMSD3* were only detected in trace amounts in some fruit tissues (Table S4). By comparing the total expression of *AktSODs* in flesh, seed and rind tissues, higher expression levels of *AktCSD2*, *AktCSD3*, *AktMSD1* and *AktMSD4* in flesh were observed; *AktCSD1*, *AktCSD4* and *AktCSD5* showed slightly higher expression levels in seeds, and only *AktCSD6* displayed higher expression

in rinds (Figure 5b). Overall, expression levels of *AktFSD1* and *AktFSD2* were extremely similar in the three fruit tissues (Figure 5b).

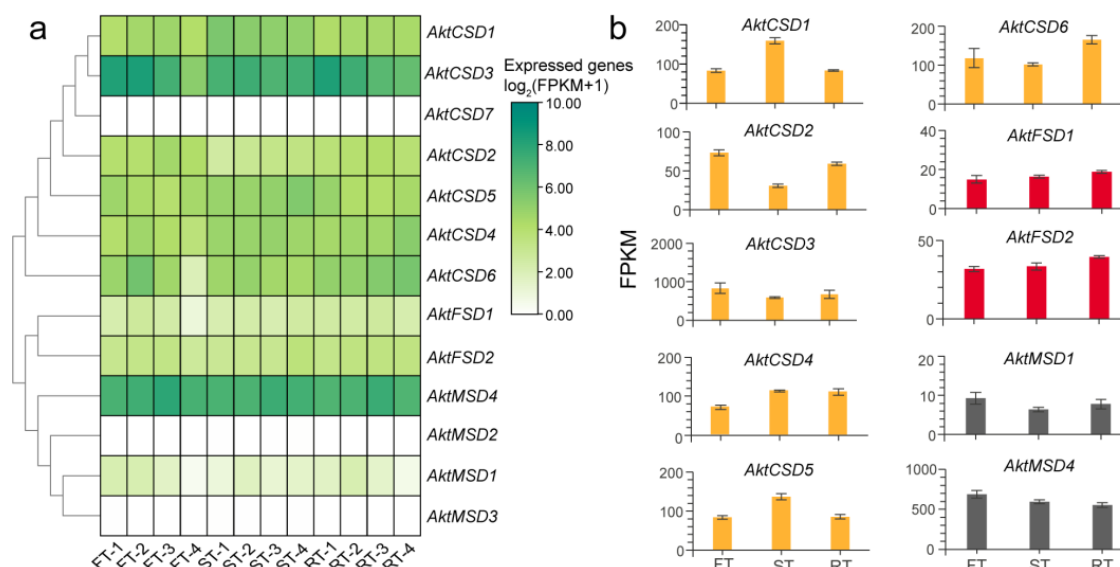


**Figure 5.** Expression levels of 13 *AktSODs* in different tissues and developmental stages (FT: flesh, ST: seed, RT: rind, 1: young stage, 2: enlargement stage, 3: coloring stage, 4: mature stage). (a) Heatmap of expression of 13 *AktSODs* in three fruit tissues at four stages. (b) Total expression of *AktSODs* in three fruit tissues contains the total FPKM of each fruit tissue in its four development stages. The error bars of the column represent the standard deviation of FPKM in the four development stages. The different colors of the column represent three subfamilies of *AktSODs*.

### 3.7. Metabolic Regulatory Network Involved in *AktSODs* in Fruit Development

We performed WGCNA on 12 transcriptome datasets during fruit development of *A. trifoliata*, and found that *AktSODs* participate in the metabolic regulatory network. The genes expressed in the transcriptomes after filtering low-expression genes were divided into 18 modules (Figure S1); 9 *AktSODs* were assigned to 6 modules, and the remaining 4 *AktSODs* were excluded due to low expression or no expression in fruit tissues. *AktFSD1*, *AktFSD2* and *AktCSD6* were assigned to the same module. *AktCSD1* and *AktCSD2* were assigned to another module, and the remaining 4 *AktSODs* were assigned to four different modules.

We further focused on the set of genes expressed in association with the 9 *AktSODs* from the module in which the *AktSODs* are located (Table S5). GO enrichment analysis was performed on the 9 *AktSOD*-associated gene sets, and the results are illustrated in Figure 6. The *AktSOD* genes assigned to the same module collectively participate in a large number of identical metabolic networks, but there are also differences. For example, the gene sets associated with the expression levels of *AktCSD1* and *AktCSD2* were enriched in the negative regulation of gene expression and chromatin organization. Conversely, *AktCSD1*-related genes were more assigned to the negative regulation of macromolecule metabolic processes, unlike *AktCSD2*. The gene sets associated with the expression levels of *AktFSD1*, *AktFSD2* and *AktCSD6* were all enriched in the obsolete cytoplasmic part and ribosomal subunit, and the metabolic network involving *AktFSD1* and *AktFSD2* was more similar than that of *AktCSD6*. In addition, it is worth noting that the gene set associated with the expression level of *AktCSD4* is associated with the response to stress, and that the gene set associated with the expression level of *AktMSD4* is related to fruit development.



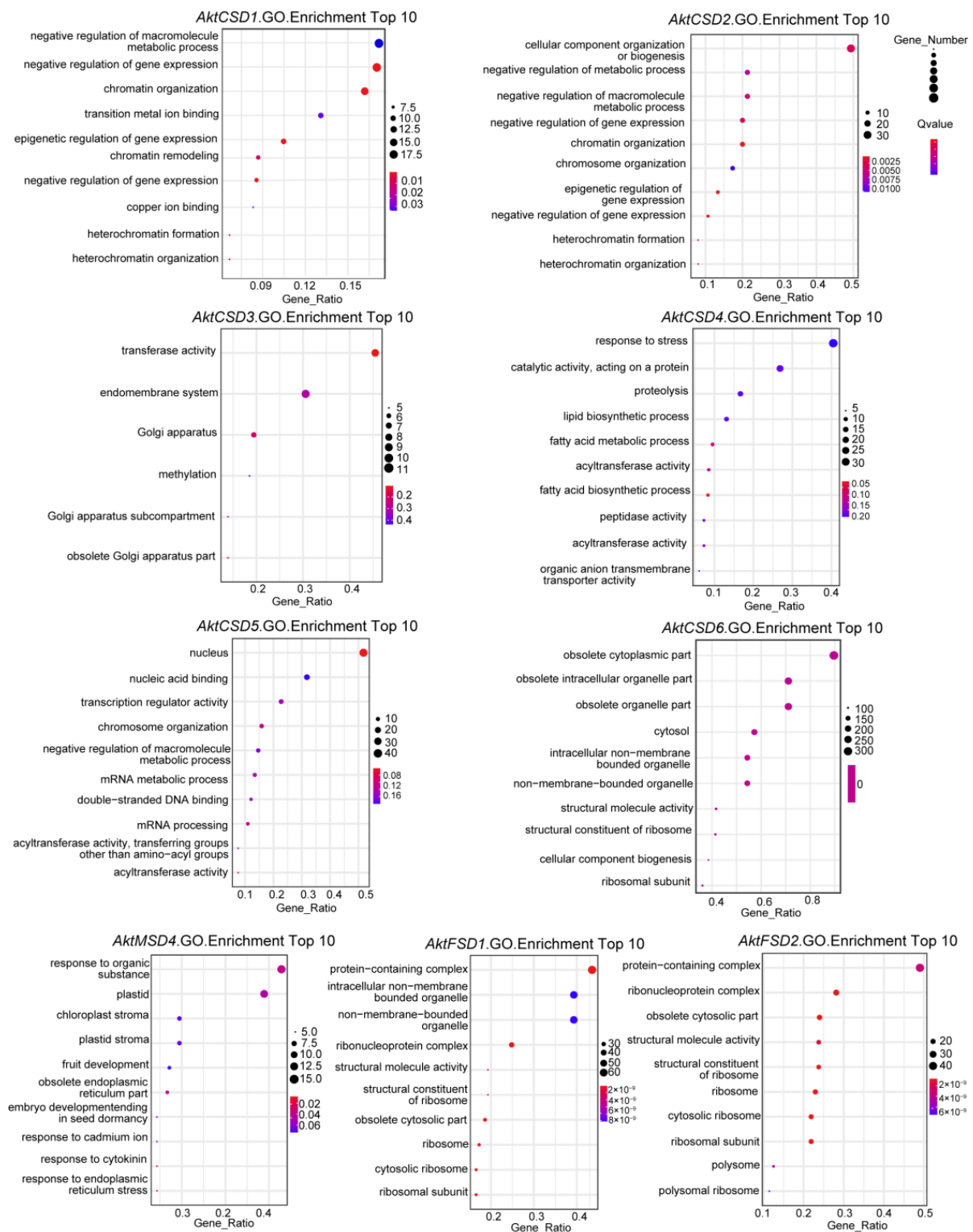


**Figure 6.** GO enrichment analysis of gene sets associated with *AktSOD* expression.

### 3.8. Differential Expression of *AktSODs* in Resistant and Susceptible Rinds

Transcriptome data for rind tissues with different disease resistance levels were used to explore the expression of *AktSODs* in response to various pathogenic bacteria. By comparing the expression levels of *AktSODs* in resistant rinds (a mixed pool of 24 lines) and susceptible rinds (a mixed pool of 50 lines), it was found that almost all *AktSODs* were significantly expressed in resistant or susceptible rinds, except for *AktCSD7* (Figure 7;

Table S6). Among the 12 *AktSODs*, *AktCSD2*, *AktFSD1*, and *AktFSD2* showed more drastic upregulation in resistant rinds during the period of rapid fruit expansion than in susceptible lines. In addition, the three *MnSODs* (*AktMSD1*, *AktMSD2* and *AktMSD3*) were rapidly upregulated in resistant rinds, with extremely weak or even no expression in susceptible rinds.

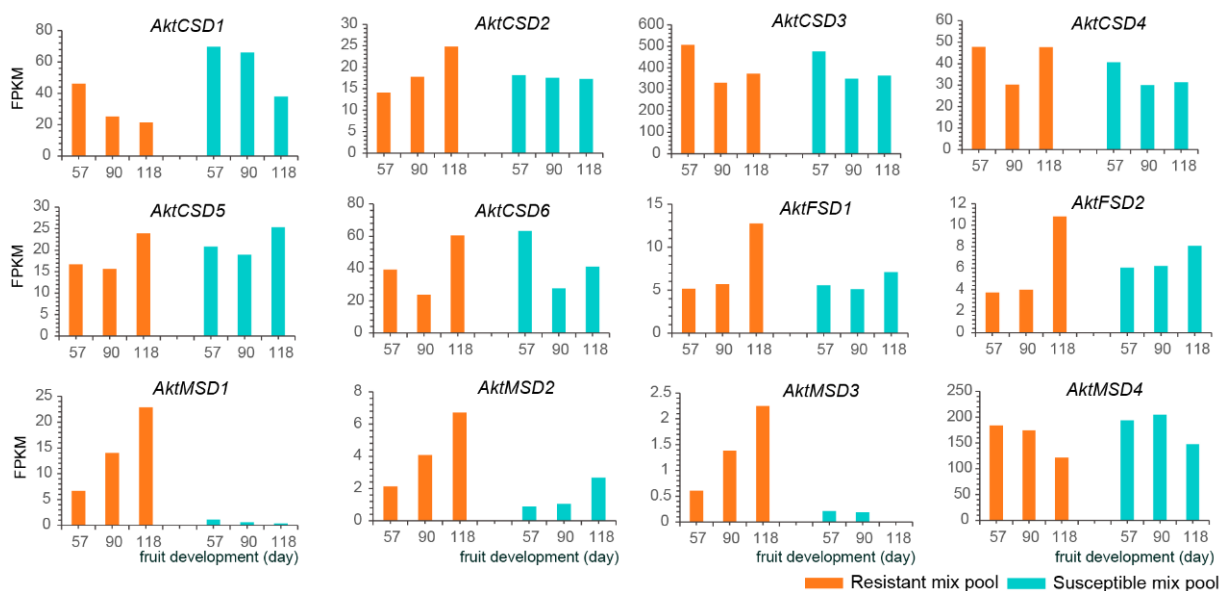


**Figure 7.** Expression-level analysis of 13 *AktSODs* in resistant and susceptible rinds.

#### 4. Discussion

*A. trifoliata* is a newly domesticated fruit tree, horticultural crop and potential oil crop [37]. Abiotic and biotic stresses are the main factors that cause serious declines in the fruit yield and quality of artificially cultivated *A. trifoliata*. *SOD* genes have been reported to play a crucial role in biotic stress, abiotic stress and fruit growth and development. In our current research, the reference genome and transcriptome data available for *A. trifoliata* provided an opportunity to explore the function of *AktSODs* and their expression in response to fruit development and biotic stress.

##### 4.1. The *AktSOD* Family Is Highly Conserved during Evolutionary Adaptation

In the current study, we identified 13 *SOD* genes in the *A. trifoliata* genome, including 2 *FeSODs*, 4 *MnSODs* and 7 *Cu/ZnSODs*. Similar to most angiosperms, the number of *AktSOD* family members is highly conserved in evolution, with almost no large-scale expansion, such as the 7 *SOD* genes in barley [38] and *A. thaliana* [39], the 9 *SOD* genes in tomato [40], the 10 *SOD* genes in grapevine [41], the 13 *SOD* genes in maize [42], and the 26 *SOD* genes in wheat [43]. The three *AktSOD* subfamilies are also highly conserved with regard to gene structure. *Akt-FeSODs*, *Akt-MnSODs* and *Akt-Cu/ZnSODs* include different motifs in their protein sequences, with a bias observed (Figure 2c). Gain and loss of introns/exons is a driving force of gene evolution [44]. Unlike the *SOD* genes of the tea plant [45] and rapeseed [46], the number of introns/exons of *AktSOD* genes has changed only slightly, especially in the same subfamily (Table 1). The intron–exon pattern of *AktSODs* also indicates their conservation in the evolutionary process.

Evolutionarily, different types of gene duplication may occur along different evolutionary trajectories, and may be preserved in a biased manner in different types of gene families [47]. In *A. trifoliata*, 5 (38.5%) *AktSODs* derived from genome-wide duplication events, among which 4 pairs of homologous *Cu/ZnSODs* show collinearity (Figure 3); the remaining 8 (61.5%) *AktSODs* derived from dispersed duplications (Table 1). It is worth noting that two WGD events occurred in the *A. trifoliata* genome for adaptation to drastic

changes in the environment [48]. In *A. trifoliata*, the strong WGD only expanded *Cu/ZnSOD* genes by a few copies, whereas *FeSODs* and *MnSODs* appear to have been unaffected by WGD. This evolutionary evidence further demonstrates that *AktSODs* are highly conserved.

#### 4.2. *AktSODs* Are Largely Functionally Diverse and Widely Involved in *A. trifoliata* Fruit Development

Overall, the physical properties of proteins play an important role in determining the biochemical function of the molecule [49]. Physical characterization of *SOD* proteins showed extensive differences in protein sequence length, isoelectric point and molecular weight in the 13 *AktSOD* proteins (Table 1). Further focusing on cis-elements in their promoter regions revealed a large number of light-responsive and hormone-responsive elements distributed in the 13 *AktSODs* (Figure 4). The abundant environmental and plant hormone-responsive elements in *AktSOD* promoters may be related to different roles or regulatory mechanisms in response to biotic and abiotic stresses. In addition, great variation in number and type exists, and some elements responding to metabolism and gene expression are specific to some *SOD* genes. For example, 6 (46.15%) *AktSODs* have meristem expression responsive cis-elements, but 5 (38.16%) *AktSODs* lack transcriptional activator responsive cis-elements (Figure 4). In general, differences in the structure of *AktSODs* may cause changes in protein function.

Differences in expression levels and tissue specificity of a gene family are often associated with functional differentiation [50]. Gene expression analysis showed 12 (92.31%) of the *AktSODs* to be involved in fruit growth and development. *AktCSD3* and *AktMSD4* were persistently expressed at high levels in flesh, seed and rind tissues, whereas *AktMSD2* and *AktMSD3* showed spatiotemporally specific expression during fruit development. Such specific expression of *AktSODs* indicates that they are involved in different physiological activities.

In previous studies, it has been reported that the main function of *SOD* genes is to respond extensively to various abiotic stresses [45], and increasing *SOD* activity is an effective way to improve stress resistance in plants [51,52]. However, in the process of fruit development, ROS is continuously released during vigorous metabolic activities [53], and the surface of the fruit is also attacked by various pathogenic bacteria, so the *SOD* genes also play an important role in the process of fruit development. In the current study, WGCNA of transcriptome data further revealed that these *AktSODs* participate in distinct metabolic networks during fruit development. First, the 9 (69.23%) *AktSODs* included in the analysis were assigned to 6 modules, and expression levels of 5 (39.46%) *AktSODs* were associated with other *SOD* genes, suggesting a cooperative division of labor between *AktSOD* genes. Second, the gene sets associated with *AktSODs* were enriched in different molecular function, biological process and cellular component networks, also confirming that the metabolic network pathways regulated by *AktSODs* are different. Through enrichment analysis, we also inferred that *AktCSD4* is extremely likely to be involved in the stress response, and that *AktMSD4* may be involved in the regulation of fruit development because the associated expression gene set was enriched in the corresponding pathway.

#### 4.3. Three *MnSODs* May Play an Important Role in Resisting Invasion of Pathogenic Bacteria

The relationship between *SODs* and plant disease resistance has been extensively studied due to its focus on the regulation of endogenous ROS [54]. A large number of reports indicate that some *SOD* genes can enhance the resistance of plants to specific pathogens. For example, tobacco has been transformed with a *Cu/ZnSOD* gene from *Spinacia oleracea*, not only improving its tolerance to water stress but also its resistance to *Pseudomonas syringae* pv. *tabaci* [55]. Another study reported that after a *MnSOD* gene derived from oil radish was transferred to broccoli, the transgenic lines showed a higher resistance to downy mildew [56]. Comparing expression levels of *SOD* genes in the rinds of various resistant and susceptible lines, we found that some *SOD* genes may be induced by

pathogenic bacteria under natural conditions. For instance, 3 *Akt-MnSOD* genes, *AktMSD1*, *AktMSD2* and *AktMSD3*, were expressed at very low levels or even not expressed during the development of fruit tissues and in susceptible rinds, but they were stably upregulated in resistant rinds (Figure 7). Such inducible expression of these 3 *MnSOD* genes in resistant rinds suggests that they might play an important role in the defense against pathogenic bacteria.

## 5. Conclusions

In this bioinformatics study, a total of 13 *SODs* classified into three categories were identified in the reference genome of *A. trifoliata*. The phylogeny, motif composition, intron–exon pattern and replication type of the *AktSODs* all indicate that these *SODs* of *A. trifoliata* are extremely conserved in the evolutionary process, and that only a few copies have undergone expansion by segmental duplication/WGD and dispersed duplication. WGCNA of the transcriptome of *A. trifoliata* fruit revealed the metabolic network in which *AktSOD* genes may be involved during fruit development, with *AktMSD4* being involved in responding to stress and *AktCSD4* possibly regulating fruit development. Comparing the expression of *AktSOD* genes in resistant and susceptible rinds, it was found that *AktMSD1*, *AktMSD2* and *AktMSD3* are induced by pathogens and may be involved in defense against these organisms. Overall, this study lays the foundation for improving biotic and abiotic stress responses of *A. trifoliata* and provides information on the regulation of *AktSOD* gene expression, especially during fruit development.

**Supplementary Materials:** The following supporting information can be downloaded at <https://www.mdpi.com/article/10.3390/antiox12030726/s1>, Figure S1: WGCNA of the fruit developmental transcriptome; Table S1: *SOD* sequences in four different evolutionary node species; Table S2: The information of identified 10 motifs in *AktSOD* proteins; Table S3: Detailed information of cis-acting elements in the 2000 bp region of *SOD* gene coding regions; Table S4: The expression level of 13 *SOD* genes in the fruit transcriptome of *A. trifoliata*; Table S5: List of genes expressed in association with *AktSOD* genes in the same module; Table S6: The expression level of *SOD* genes in resistant and susceptible rinds of *A. trifoliata*.

**Author Contributions:** Conceptualization, H.Y. (Huai Yang), G.C. and P.L.; methodology, H.Y. (Huai Yang), Q.Z. and S.Z.; software, Q.Z., H.Y. (Huai Yang) and H.Y. (Hao Yang); validation, C.C., F.T. and T.R.; formal analysis, H.Y. (Huai Yang); resources, P.L.; data curation, H.Y. (Huai Yang) and S.Z.; writing—original draft preparation, H.Y. (Huai Yang); writing—review and editing, H.Y. (Huai Yang) and P.L.; visualization, H.Y. (Huai Yang); supervision, J.L., T.R. and F.T.; project administration, P.L.; funding acquisition, P.L. All authors have read and agreed to the published version of the manuscript.

**Funding:** This research was supported by the Science and Technology Department of Sichuan Province, grant numbers 2020YFN0057 and 2022ZHXC0002, and the Bureau of Science and Technology of Chengdu, grant numbers 2021-YF05-01863-SN and 2021-YF05-01328-SN.

**Institutional Review Board Statement:** Not applicable.

**Informed Consent Statement:** Not applicable.

**Data Availability Statement:** All data analyzed during this study are included in the manuscript and Supplementary Information files. Genome sequence files of *A. trifoliata* were downloaded from the National Genomics Data Center database under BioProject PRJCA003847. Transcriptome data for *A. trifoliata* were downloaded from the NCBI database under accession numbers PRJNA671772, SAMN16551931–33, SAMN16551934–36, SAMN16551937–39, SAMN16551940–42 and the National Genomics Data Center database under BioProject PRJCA014987.

**Acknowledgments:** We are grateful to the Science and Technology Department of Sichuan Province and the Bureau of Science and Technology of Chengdu for supporting this study.

**Conflicts of Interest:** The authors declare no conflict of interest.

## References

1. Mittler, R. Oxidative stress, antioxidants and stress tolerance. *Trends Plant Sci.* **2002**, *7*, 405–410. [[CrossRef](#)] [[PubMed](#)]
2. Rizhsky, L.; Liang, H.; Shuman, J.; Shulaev, V.; Davletova, S.; Mittler, R. When defense pathways collide. The response of Arabidopsis to a combination of drought and heat stress. *Plant Physiol.* **2004**, *134*, 1683–1696. [[CrossRef](#)] [[PubMed](#)]
3. Sarvajeet, S.G.; Narendra, T. Reactive oxygen species and antioxidant machinery in abiotic stress tolerance in crop plants. *Plant Physiol. Biochem.* **2010**, *48*, 909–930. [[CrossRef](#)]
4. Balint-Kurti, P. The plant hypersensitive response: Concepts, control and consequences. *Mol. Plant Pathol.* **2019**, *20*, 1163–1178. [[CrossRef](#)]
5. Tyagi, S.; Shah, A.; Karthik, K.; Rathinam, M.; Rai, V.; Chaudhary, N.; Sreevathsa, R. Reactive oxygen species in plants: An invincible fulcrum for biotic stress mitigation. *Appl. Microbiol. Biotechnol.* **2022**, *106*, 5945–5955. [[CrossRef](#)]
6. Hernández, J.A.; Ferrer, M.A.; Jiménez, A.; Barceló, A.R.; Sevilla, F. Antioxidant Systems and O<sub>2</sub><sup>-</sup>/H<sub>2</sub>O<sub>2</sub> Production in the apoplast of pea leaves. Its relation with salt-induced necrotic lesions in minor veins. *Plant Physiol.* **2001**, *127*, 817–831. [[CrossRef](#)]
7. Abreu, I.A.; Cabelli, D.E. Superoxide dismutases—A review of the metal-associated mechanistic variations. *Biochim. Biophys. Acta BBA Proteins Proteom.* **2010**, *1804*, 263–274. [[CrossRef](#)]
8. Fink, R.C.; Scandalios, J.G. Molecular evolution and structure–function relationships of the superoxide dismutase gene families in angiosperms and their relationship to other eukaryotic and prokaryotic superoxide dismutases. *Arch. Biochem. Biophys.* **2002**, *399*, 19–36. [[CrossRef](#)]
9. Verma, D.; Lakhanpal, N.; Singh, K. Genome-wide identification and characterization of abiotic-stress responsive SOD (superoxide dismutase) gene family in *Brassica juncea* and *B. rapa*. *BMC Genom.* **2019**, *20*, 227. [[CrossRef](#)]
10. Zelko, I.N.; Mariani, T.J.; Folz, R.J. Superoxide dismutase multigene family: A comparison of the CuZn-SOD (SOD1), Mn-SOD (SOD2), and EC-SOD (SOD3) gene structures, evolution, and expression. *Free Radical Bio. Med.* **2002**, *33*, 337–349. [[CrossRef](#)]
11. Schmidt, A.; Gube, M.; Schmidt, A.; Kothe, E. In silico analysis of nickel containing superoxide dismutase evolution and regulation. *J. Basic Microb.* **2009**, *49*, 109–118. [[CrossRef](#)]
12. Del Río, L.A.; Corpas, F.J.; López-Huertas, E.; Palma, J.M. Plant Superoxide Dismutases: Function Under Abiotic Stress Conditions. In *Antioxidants and Antioxidant Enzymes in Higher Plants*; Gupta, D.K., Palma, J.M., Corpas, F.J., Eds.; Springer International Publishing: Berlin, Germany, 2018; pp. 1–26. ISBN 978-3-319-75087-3. [[CrossRef](#)]
13. Miller, A. Superoxide dismutases: Ancient enzymes and new insights. *FEBS Lett.* **2012**, *586*, 585–595. [[CrossRef](#)]
14. Filiz, E.; Koc, I.; Ozyigit, I.I. Comparative analysis and modeling of superoxide dismutases (SODs) in *Brachypodium distachyon* L. *Appl. Biochem. Biotechnol.* **2014**, *173*, 1183–1196. [[CrossRef](#)]
15. Amo, T.; Atomi, H.; Imanaka, T. Biochemical properties and regulated gene expression of the superoxide dismutase from the facultatively aerobic hyperthermophile *Pyrobaculum calidifontis*. *J. Bacteriol.* **2003**, *185*, 6340–6347. [[CrossRef](#)]
16. Nakamura, T.; Torikai, K.; Uegaki, K.; Morita, J.; Machida, K.; Suzuki, A.; Kawata, Y. Crystal structure of the cambialistic superoxide dismutase from *Aeropyrum pernix* K1—insights into the enzyme mechanism and stability. *FEBS J.* **2011**, *278*, 598–609. [[CrossRef](#)]
17. Pilon, M.; Ravet, K.; Tapken, W. The biogenesis and physiological function of chloroplast superoxide dismutases. *Biochim. Biophys. Acta BBA Bioenerg.* **2011**, *1807*, 989–998. [[CrossRef](#)]
18. Jalali-E-Emam, S.M.S.; Alizadeh, B.; Zaefizadeh, M.; Zakarya, R.A.; Khayatnezhad, M. Superoxide dismutase (SOD) activity in NaCl stress in salt-sensitive and salt-tolerance genotypes of Colza (*Brassica napus* L.). *Middle East J. Sci. Res.* **2011**, *7*, 7–11.
19. Wang, L.; Yao, L.; Hao, X.; Li, N.; Wang, Y.; Ding, C.; Lei, L.; Qian, W.; Zeng, J.; Yang, Y.; et al. Transcriptional and physiological analyses reveal the association of ROS metabolism with cold tolerance in tea plant. *Environ. Exp. Bot.* **2019**, *160*, 45–58. [[CrossRef](#)]
20. Tertivanidis, K.; Goudoula, C.; Vasilikiotis, C.; Hassiotou, E.; Perl-Treves, R.; Tsafaris, A. Superoxide dismutase transgenes in sugarbeets confer resistance to oxidative agents and the fungus *C. beticola*. *Transgenic Res.* **2004**, *13*, 225–233. [[CrossRef](#)]
21. Abassi, N.A.; Kushad, M.M.; Endress, A.G. Active oxygen-scavenging enzymes activities in developing apple flowers and fruits. *Sci. Hortic.* **1998**, *74*, 183–194. [[CrossRef](#)]
22. Lv, J.; Zhang, J.; Han, X.; Bai, L.; Xu, D.; Ding, S.; Ge, Y.; Li, C.; Li, J. Genome wide identification of superoxide dismutase (SOD) genes and their expression profiles under 1-methylcyclopropene (1-MCP) treatment during ripening of apple fruit. *Sci. Hortic.* **2020**, *271*, 109471. [[CrossRef](#)]
23. Jiang, Y.; Ding, Y.; Wang, D.; Deng, Y.; Zhao, Y. Radio frequency-assisted enzymatic extraction of anthocyanins from *Akebia trifoliata* (Thunb.) Koidz. flowers: Process optimization, structure, and bioactivity determination. *Ind. Crops Prod.* **2020**, *149*, 112327. [[CrossRef](#)]
24. Du, Y.; Jiang, Y.; Zhu, X.; Xiong, H.; Shi, S.; Hu, J.; Peng, H.; Zhou, Q.; Sun, W. Physicochemical and functional properties of the protein isolate and major fractions prepared from *Akebia trifoliata* var. australis seed. *Food Chem.* **2012**, *133*, 923–929. [[CrossRef](#)]
25. Niu, J.; Shi, Y.; Huang, K.; Zhong, Y.; Chen, J.; Sun, Z.; Luan, M.; Chen, J. Integrative transcriptome and proteome analyses provide new insights into different stages of *Akebia trifoliata* fruit cracking during ripening. *Biotechnol. Biofuels* **2020**, *13*, 149. [[CrossRef](#)] [[PubMed](#)]
26. Kourelis, J.; van der Hoorn, R.A.L. Defended to the nines: 25 years of resistance gene cloning identifies nine mechanisms for R protein function. *Plant Cell* **2018**, *30*, 285–299. [[CrossRef](#)] [[PubMed](#)]
27. Yu, X.; Zhong, S.; Yang, H.; Chen, C.; Chen, W.; Yang, H.; Guan, J.; Fu, P.; Tan, F.; Ren, T.; et al. Identification and characterization of NBS resistance genes in *Akebia trifoliata*. *Front. Plant Sci.* **2021**, *12*, 758559. [[CrossRef](#)]

28. El-Gebali, S.; Mistry, J.; Bateman, A.; Eddy, S.R.; Luciani, A.; Potter, S.C.; Qureshi, M.; Richardson, L.J.; Salazar, G.A.; Smart, A.; et al. The Pfam protein families database in 2019. *Nucleic Acids Res.* **2019**, *47*, D427–D432. [[CrossRef](#)]
29. Tamura, K.; Stecher, G.; Kumar, S. MEGA11: Molecular evolutionary genetics analysis version 11. *Mol. Biol. Evol.* **2021**, *38*, 3022–3027. [[CrossRef](#)]
30. Chen, C.; Chen, H.; Zhang, Y.; Thomas, H.R.; Frank, M.H.; He, Y.; Xia, R. TBtools: An integrative toolkit developed for interactive analyses of big biological data. *Mol. Plant* **2020**, *13*, 1194–1202. [[CrossRef](#)]
31. Nguyen, L.; Schmidt, H.A.; von Haeseler, A.; Minh, B.Q. IQ-TREE: A fast and effective stochastic algorithm for estimating maximum-likelihood phylogenies. *Mol. Biol. Evol.* **2015**, *32*, 268–274. [[CrossRef](#)]
32. Letunic, I.; Bork, P. Interactive tree of life (iTOL) v4: Recent updates and new developments. *Nucleic Acids Res.* **2019**, *47*, W256–W259. [[CrossRef](#)]
33. Lescot, M.; Déhais, P.; Thijs, G.; Marchal, K.; Moreau, Y.; Van de Peer, Y.; Rouzé, P.; Rombauts, S. PlantCARE, a database of plant cis-acting regulatory elements and a portal to tools for in silico analysis of promoter sequences. *Nucleic Acids Res.* **2002**, *30*, 325–327. [[CrossRef](#)]
34. Perteira, M.; Kim, D.; Perteira, G.M.; Leek, J.T.; Salzberg, S.L. Transcript-level expression analysis of RNA-seq experiments with HISAT, StringTie and Ballgown. *Nat. Protoc.* **2016**, *11*, 1650–1667. [[CrossRef](#)]
35. Love, M.I.; Huber, W.; Anders, S. Moderated estimation of fold change and dispersion for RNA-seq data with DESeq2. *Genome Biol.* **2014**, *15*, 550. [[CrossRef](#)]
36. Powell, S.; Forslund, K.; Szklarczyk, D.; Trachana, K.; Roth, A.; Huerta-Cepas, J.; Gabaldón, T.; Rattei, T.; Creevey, C.; Kuhn, M.; et al. eggNOG v4.0: Nested orthology inference across 3686 organisms. *Nucleic Acids Res.* **2014**, *42*, D231–D239. [[CrossRef](#)]
37. Guan, J.; Fu, P.; Wang, X.; Yu, X.; Zhong, S.; Chen, W.; Yang, H.; Chen, C.; Yang, H.; Luo, P. Assessment of the breeding potential of a set of genotypes selected from a natural population of *Akebia trifoliata* (Three-Leaf Akebia). *Horticulturae* **2022**, *8*, 116. [[CrossRef](#)]
38. Zhang, X.; Zhang, L.; Chen, Y.; Wang, S.; Fang, Y.; Zhang, X.; Wu, Y.; Xue, D. Genome-wide identification of the SOD gene family and expression analysis under drought and salt stress in barley. *Plant Growth Regul.* **2021**, *94*, 49–60. [[CrossRef](#)]
39. Gharari, Z.; Nejad, R.K.; Band, R.S.; Najafi, F.; Nabiuni, M.; Irian, S. The role of *Mn-SOD* and *Fe-SOD* genes in the response to low temperature in chs mutants of *Arabidopsis*. *Turk. J. Bot.* **2014**, *38*, 80–88. [[CrossRef](#)]
40. Feng, K.; Yu, J.; Cheng, Y.; Ruan, M.; Wang, R.; Ye, Q.; Zhou, G.; Li, Z.; Yao, Z.; Yang, Y.; et al. The SOD gene family in tomato: Identification, phylogenetic relationships, and expression patterns. *Front. Plant Sci.* **2016**, *7*, 1279. [[CrossRef](#)]
41. Hu, X.; Hao, C.; Cheng, Z.; Zhong, Y.; Corrado, G. Genome-wide identification, characterization, and expression analysis of the grapevine superoxide dismutase (SOD) Family. *Int. J. Genom.* **2019**, *2019*, 7350414. [[CrossRef](#)]
42. Liu, J.; Xu, L.; Shang, J.; Hu, X.; Yu, H.; Wu, H.; Lv, W.; Zhao, Y. Genome-wide analysis of the maize superoxide dismutase (SOD) gene family reveals important roles in drought and salt responses. *Genet. Mol. Biol.* **2021**, *44*, e20210035. [[CrossRef](#)] [[PubMed](#)]
43. Jiang, W.; Yang, L.; He, Y.; Zhang, H.; Li, W.; Chen, H.; Ma, D.; Yin, J. Genome-wide identification and transcriptional expression analysis of superoxide dismutase (SOD) family in wheat (*Triticum aestivum*). *PeerJ* **2019**, *7*, e8062. [[CrossRef](#)] [[PubMed](#)]
44. Xu, G.; Guo, C.; Shan, H.; Kong, H. Divergence of duplicate genes in exon–intron structure. *Proc. Natl. Acad. Sci. USA* **2012**, *109*, 1187–1192. [[CrossRef](#)] [[PubMed](#)]
45. Zhou, C.; Zhu, C.; Fu, H.; Li, X.; Chen, L.; Lin, Y.; Lai, Z.; Guo, Y. Genome-wide investigation of superoxide dismutase (SOD) gene family and their regulatory miRNAs reveal the involvement in abiotic stress and hormone response in tea plant (*Camellia sinensis*). *PLoS ONE* **2019**, *14*, e223609. [[CrossRef](#)] [[PubMed](#)]
46. Su, W.; Raza, A.; Gao, A.; Jia, Z.; Zhang, Y.; Hussain, M.A.; Mehmood, S.S.; Cheng, Y.; Lv, Y.; Zou, X. Genome-wide analysis and expression profile of superoxide dismutase (SOD) gene family in Rapeseed (*Brassica napus* L.) under different hormones and abiotic stress conditions. *Antioxidants* **2021**, *10*, 1182. [[CrossRef](#)]
47. Qiao, X.; Yin, H.; Li, L.; Wang, R.; Wu, J.; Wu, J.; Zhang, S. Different modes of gene duplication show divergent evolutionary patterns and contribute differently to the expansion of gene families involved in important fruit traits in Pear (*Pyrus bretschneideri*). *Front. Plant Sci.* **2018**, *9*, 161. [[CrossRef](#)]
48. Zhong, S.; Li, B.; Chen, W.; Wang, L.; Guan, J.; Wang, Q.; Yang, Z.; Yang, H.; Wang, X.; Yu, X.; et al. The chromosome-level genome of *Akebia trifoliata* as an important resource to study plant evolution and environmental adaptation in the Cretaceous. *Plant J.* **2022**, *112*, 1316–1330. [[CrossRef](#)]
49. Mohanta, T.K.; Khan, A.; Hashem, A.; Abd Allah, E.F.; Al-Harrasi, A. The molecular mass and isoelectric point of plant proteomes. *BMC Genom.* **2019**, *20*, 631. [[CrossRef](#)]
50. Hunt, L.; Otterhag, L.; Lee, J.C.; Lasheen, T.; Hunt, J.; Seki, M.; Shinozaki, K.; Sommarin, M.; Gilmour, D.J.; Pical, C.; et al. Gene-specific expression and calcium activation of *Arabidopsis thaliana* phospholipase C isoforms. *New Phytol.* **2004**, *162*, 643–654. [[CrossRef](#)]
51. Wang, F.; Wang, Q.; Kwon, S.; Kwak, S.; Su, W. Enhanced drought tolerance of transgenic rice plants expressing a pea manganese superoxide dismutase. *J. Plant Physiol.* **2005**, *162*, 465–472. [[CrossRef](#)]
52. Zhang, D.; Yang, H.; Li, X.; Li, H.; Wang, Y. Overexpression of *Tamarix albiflorum* *TaMnSOD* increases drought tolerance in transgenic cotton. *Mol. Breed.* **2014**, *34*, 1–11. [[CrossRef](#)]
53. Tian, S.; Qin, G.; Li, B. Reactive oxygen species involved in regulating fruit senescence and fungal pathogenicity. *Plant Mol. Biol.* **2013**, *82*, 593–602. [[CrossRef](#)]

54. Wang, W.; Xia, M.X.; Chen, J.; Yuan, R.; Deng, F.N.; Shen, F.F. Gene expression characteristics and regulation mechanisms of superoxide dismutase and its physiological roles in plants under stress. *Biochemistry* **2016**, *81*, 465–480. [[CrossRef](#)]
55. Faize, M.; Burgos, L.; Faize, L.; Petri, C.; Barba-Espin, G.; Díaz-Vivancos, P.; Clemente-Moreno, M.J.; Albuquerque, N.; Hernandez, J.A. Modulation of tobacco bacterial disease resistance using cytosolic ascorbate peroxidase and Cu, Zn-superoxide dismutase. *Plant Pathol.* **2012**, *61*, 858–866. [[CrossRef](#)]
56. Jiang, M.; Miao, L.; He, C. Overexpression of an Oil Radish superoxide dismutase gene in Broccoli confers resistance to Downy Mildew. *Plant Mol. Biol. Rep.* **2012**, *30*, 966–972. [[CrossRef](#)]

**Disclaimer/Publisher’s Note:** The statements, opinions and data contained in all publications are solely those of the individual author(s) and contributor(s) and not of MDPI and/or the editor(s). MDPI and/or the editor(s) disclaim responsibility for any injury to people or property resulting from any ideas, methods, instructions or products referred to in the content.